Therapeutics and Clinical Risk Management

Dovepress
open access to scientific and medical research

Open Access Full Text Article

ORIGINAL RESEARCH

The features of cerebral permeability and perfusion detected by dynamic contrast-enhanced magnetic resonance imaging with Patlak model in relapsing–remitting multiple sclerosis

This article was published in the following Dove Medical Press journal:
Therapeutics and Clinical Risk Management

Hua Xiong[1,2]
Ping Yin[3]
Xiaojiao Li[1,2]
Chao Yang[1,2]
Dan Zhang[1,2]
Xianlong Huang[1,2]
Zhuoyue Tang[1,2]

[1]Department of Radiology, Chongqing General Hospital, University of Chinese Academy of Sciences, Chongqing 400014, China; [2]Molecular and Functional Imaging Laboratory, Chongqing General Hospital, University of Chinese Academy of Sciences, Chongqing 400014, China; [3]Department of Radiology, The First Affiliated Hospital of Chongqing Medical University, Chongqing 400016, China

Objective: To investigate the features of cerebral permeability and perfusion detected by dynamic contrast-enhanced magnetic resonance imaging (DCE-MRI) with Patlak model in relapsing–remitting multiple sclerosis (RRMS) and their correlations with Expanded Disability Status Scale (EDSS) scores and disease duration.

Patients and methods: Twenty-seven RRMS patients underwent conventional MRI and DCE-MRI with 3.0 T magnetic resonance scanner were enrolled in the study. A Patlak model was used to quantitatively measure MRI biomarkers, including volume transfer constant (K^{trans}), fractional plasma volume (V_p), cerebral blood flow (CBF), and cerebral blood volume (CBV). The correlations of MRI biomarkers with EDSS scores and disease duration were analyzed.

Results: The MRI biomarkers K^{trans}, V_p, CBF, and CBV of contrast-enhancing (CE) lesions were significantly higher ($P<0.05$) than those of non-enhancing (NE) lesions and normal-appearing white matter (NAWM) regions. The skewness and kurtosis of K^{trans} values in CE lesions were significantly higher ($P<0.05$) than that of NE lesions. No significant correlation was found among the biomarkers with EDSS scores and disease duration ($P>0.05$).

Conclusion: Our study demonstrated the abnormalities of permeability and perfusion characteristics in multiple sclerosis (MS) lesions and NAWM regions by DCE-MRI with Patlak model. The K^{trans}, V_p, CBF, and CBV of CE lesions were significantly higher than that of NE lesions, but these MRI biomarkers did not associate with the severity and duration of the disease. The skewness and kurtosis of K^{trans} value in CE lesions were significantly higher than that in NE lesions, indicating that these parameters of K^{trans} histogram can be used to distinguish the pathology of MS lesions.

Keywords: dynamic contrast-enhanced magnetic resonance imaging, Patlak model, multiple sclerosis, permeability, perfusion, histogram

Introduction

Dynamic contrast-enhanced magnetic resonance imaging (DCE-MRI) is increasingly used to quantitatively assess the permeability and perfusion of subtle microvascular environment.[1,2] This technique was originally developed to estimate the blood–brain barrier (BBB) permeability in brain tumors.[3–5] Many studies have shown the abnormalities of BBB in multiple sclerosis (MS).[3,4,6–10] MS disrupts the integrity of BBB enabling active components of the immune system to enter the brain parenchyma to form the focal lesions, which is the early pathological change in MS and can be early detected by DCE-MRI.[8] Diverse pathological changes were shown in different lesions

Correspondence: Zhuoyue Tang
Department of Radiology, Chongqing General Hospital, University of Chinese Academy of Sciences, 104 Pipashan Main St, Yuzhong District, Chongqing 400014, China
Email zhuoyue_tang@cqmu.edu.cn

submit your manuscript | www.dovepress.com
Dovepress
http://dx.doi.org/10.2147/TCRM.S189598

of MS.[6,9,11] The detection of spatiotemporal features of the lesions is essential for making an early and accurate diagnosis for MS patients. Recently, only a few studies have focused on both the cerebral permeability and perfusion abnormalities in MS, and the abnormalities of permeability and perfusion were observed in inactive MS lesions as well as normal-appearing white matter (NAWM) regions.[4,7,8,11,12] Therefore, it is necessary for us to study the features of permeability and perfusion in active, inactive lesions and NAWM lesions of MS with DCE-MRI.

The Patlak model is a one-compartment linear model, which assumes that the rate constant between extracellular extravascular space and blood plasma (K_{ep}) can be ignored because of low permeability and short measuring time.[13] It can offer an easily visualized demonstration of the goodness of the fit.[2,14] Histogram analysis is useful for describing the number of pixels in whole image having the same intensity.[15] Until now, number of studies used histogram approaches to improve the heterogeneity of tumors. Shukla-Dave et al[16] used this methodology to investigate the distributions of the permeability parameters of head and neck squamous cell carcinoma with DCE-MRI. Kim et al[17] calculated the histogram and permeability parameters to distinguish low- and high-grade gliomas. These studies demonstrated that the histogram parameters were significantly sensitive to small changes or treatment effects. In the present study, we tried to apply the heterogeneity of histogram to distinguish MS lesions.

Our study hypothesized that the permeability, perfusion, and histogram parameters of lesions and NAWM regions with DCE-MRI were different and can reflect different stages of MS lesions. This study investigated the application value of using DCE-MRI with Patlak model for relapsing–remitting multiple sclerosis (RRMS) by detecting MRI biomarkers, including volume transfer constant (K^{trans}), fractional plasma volume (V_p), cerebral blood flow (CBF), and cerebral blood volume (CBV) and their correlations with Expanded Disability Status Scale (EDSS) scores and disease duration.

Patients and methods

Patient populations

A total of 27 patients with clinically definite RRMS (10 males, 17 females; aged 42.9±15.6 years (range 19–78 years), median EDSS 1.0 (range 0.0–5.0), median disease duration 4.5 years (range 0.25–16.5 years) were recruited from our hospital. All patients were diagnosed based on the McDonald 2017 criteria[18] and had no other neurological diseases or psychiatric problems. No corticosteroid or immunosuppressant treatment was used for at least 3 months prior to magnetic resonance imaging (MRI) scan. This study was approved by the local Ethics Committee of Chongqing General Hospital, University of Chinese Academy of Sciences and all subjects gave written informed consent prior to participation, and this study was conducted in accordance with the Declaration of Helsinki.

Imaging data

All studies were performed on a 3.0 T MR GE Imaging System (Waukesha, WI, USA) equipped with an eight-channel phased-array head coil. The imaging protocols were as follow: 1) precontrast T_1-weighted: repetition time (TR)/echo time (TE) =1,750/24 ms, matrix size 320×224; T_2WI:TR/TE =3,900/98 ms, matrix 288×224; fluid-attenuated inversion recovery (FLAIR): TR/TE =8,000/120 ms, matrix 256×160, slice thickness/gap =5.0/0.0 mm, field of view (FOV) 24×24 cm. 2) DCE-MRI: a series of flip angle of 3°, 6°, 9°, 12°, and 15° were performed to obtain T1 mapping-based a 3D fast spoiled gradient-recalled echo. After three phases of non-enhanced (NE) acquisition, a bolus of contrast (Gadodiamide Injection, GE Healthcare, Chicago, IL, USA) was injected by an automatic double-bolus injection (Medrad, Pittsburgh, PA, USA, Spectris Solaris MR injector system) with a dose of 0.1 mmol/kg and flow rate of 2.0 mL/s followed by a 20 mL flush of saline with the same flow intravenously. The matrix size =256×160, TR/TE =6.664/2.8 ms, FOV =24×24 cm, slice thickness =5.0 mm, spatial resolution =1.5×0.9×5.0 mm, flip angle =12°. In total, 360 volumes were acquired in measurement time of 4 minutes.

Data analysis

The T2 lesion load of the patients was determined as the number of hyperintense lesions on the FLAIR images (lesions >5.0 mm) and the number of contrast-enhancing (CE) lesions was assessed on conventional T1-weighted contrast-enhanced sequences. DCE-MRI data postprocessing was performed with the Omni Kinetics software (GE Healthcare). The region of interest (ROI) was defined in the superior sagittal sinus (SSS) to measure the concentration-time curves.[19] (Figure 1) The delay between arterial and venous responses is expected to be very small compared with the temporal resolution.[20] The voxel located on the SSS was chosen to provide a high-peak signal enhancement and smooth variation during the time course. Then the contrast agent concentration was estimated.[20]

In this study, we used a Patlak model to simplify the definition of ROI in lesions and NAWM (Figure 1). ROIs were fixed in size (20–30 mm^2) and placed to CE lesions, NE lesions, and NAWM regions to acquire the

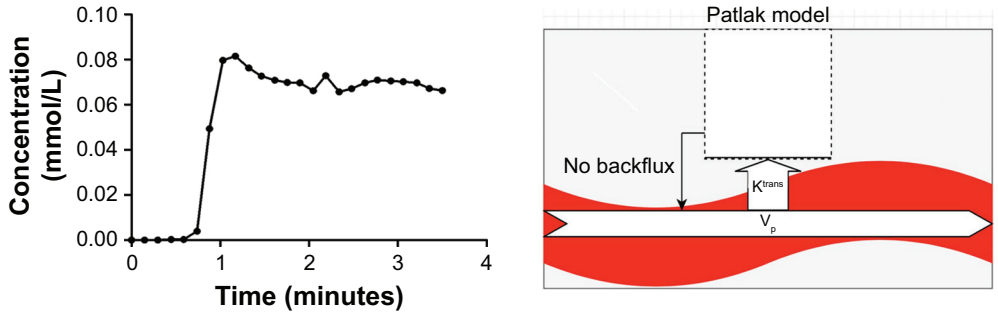

Figure 1 The time-concentration curves (left) and schematic diagram of the Patlak model (right).
Abbreviations: K^{trans}, volume transfer constant; V_p, fractional plasma volume.

MRI biomarkers, including K^{trans}, V_p, CBF, and CBV. The K^{trans} and V_p reflect the permeability characteristics of microcirculation, while CBF and CBV reflect cerebral perfusion. The artificial color mappings were performed, and the correlation among imaging biomarkers, EDSS scores, and disease duration were also analyzed. The coefficient of skewness is a measure for the degree of symmetry in the variable distribution. If skewness =0, it represents normal distribution. If skewness is <0, it represents the distribution skewed to the left, otherwise to the right. The kurtosis reflects a heavy- or light-tailed distribution. The kurtosis for a standard normal distribution is three. CE and NE lesions were measured on postcontrast T1-weighted images and precontrast FLAIR images, respectively. NAWM regions included NAWM regions near the lesions and NAWM regions far from the lesions (distance ≥5.0 mm).[21] We defined NAWM regions far from the lesions as NAWM regions on symmetrical brain avoiding arterial or venous structures to exclude the false-positive results due to physiological differences. All ROIs were handcrafted by two neuroradiologists who had >15 years of experience; discussion was done when they had different ideas.

Statistical analysis

All data were carried out by using SPSS version 21.0 software (SPSS Inc., Chicago, IL, USA). The permeability, perfusion, and histogram parameters of the lesions and NAWM regions did not conform to the normal distribution by using one-sample Kolmogorov–Smirnov test. The median (P25–P75) was used to describe these parameters. We compared the median of the K^{trans}, V_p, CBF, and CBV between groups by using Kruskal–Wallis *H* rank-sum test and Nemenyi test in SAS 9.2 software. We compared the skewness and kurtosis of MS lesions using Kruskal–Wallis *H* rank-sum test. Spearman's correlation was used to test the association of imaging biomarkers with EDSS scores and disease duration. $P<0.05$ was considered to indicate statistical significance.

Results

A total of 125 lesions were included in 27 patients with RRMS, which were mainly located in the frontal, temporal, and parietal lobes, particularly in periventricular areas (Figure 2A and B). Some lesions were found to be fused together. A total of 24 out of 27 patients were in clinical remission stage, and 3 patients were at relapse stage when the MRI examination was performed. Fourteen CE lesions were found in three patients at relapse stage, while no CE lesion was found in patients at clinical remission stage. There were no significant correlations among the K^{trans}, V_p, CBF, and CBV with EDSS scores and disease duration ($P>0.05$).

The results of permeability parameters of MS lesions and NAWM regions are shown in Figure 2C–F and Table 1. K^{trans} of CE lesions (red and yellow) were significantly higher ($P<0.05$) than those of NE lesions and the NAWM regions both near and far from lesions (green and blue) (Figure 2C). However, there was no significant difference between NE lesions and NAWM regions ($P>0.05$). V_p of CE lesions were significantly higher than those of NE lesions and NAWM regions ($P<0.05$, Figure 2D). Obvious compensatory dilation of blood vessels and collateral circulation were observed around the lesion.

The CBF and CBV of the CE lesions were notably higher than those of NE lesions and the NAWM regions both near and far from NE lesions ($P<0.05$, Figure 2E and F). In contrast, no significant difference was found in NE lesions compared with NAWM regions. The CBF and CBV of the NAWM regions close to those of NE lesions had no significant difference with the NAWM regions far from the lesions ($P>0.05$, Figure 2E and F, and Table 2). Compensatory dilation of blood vessels around the CE lesion was the same as in permeability maps.

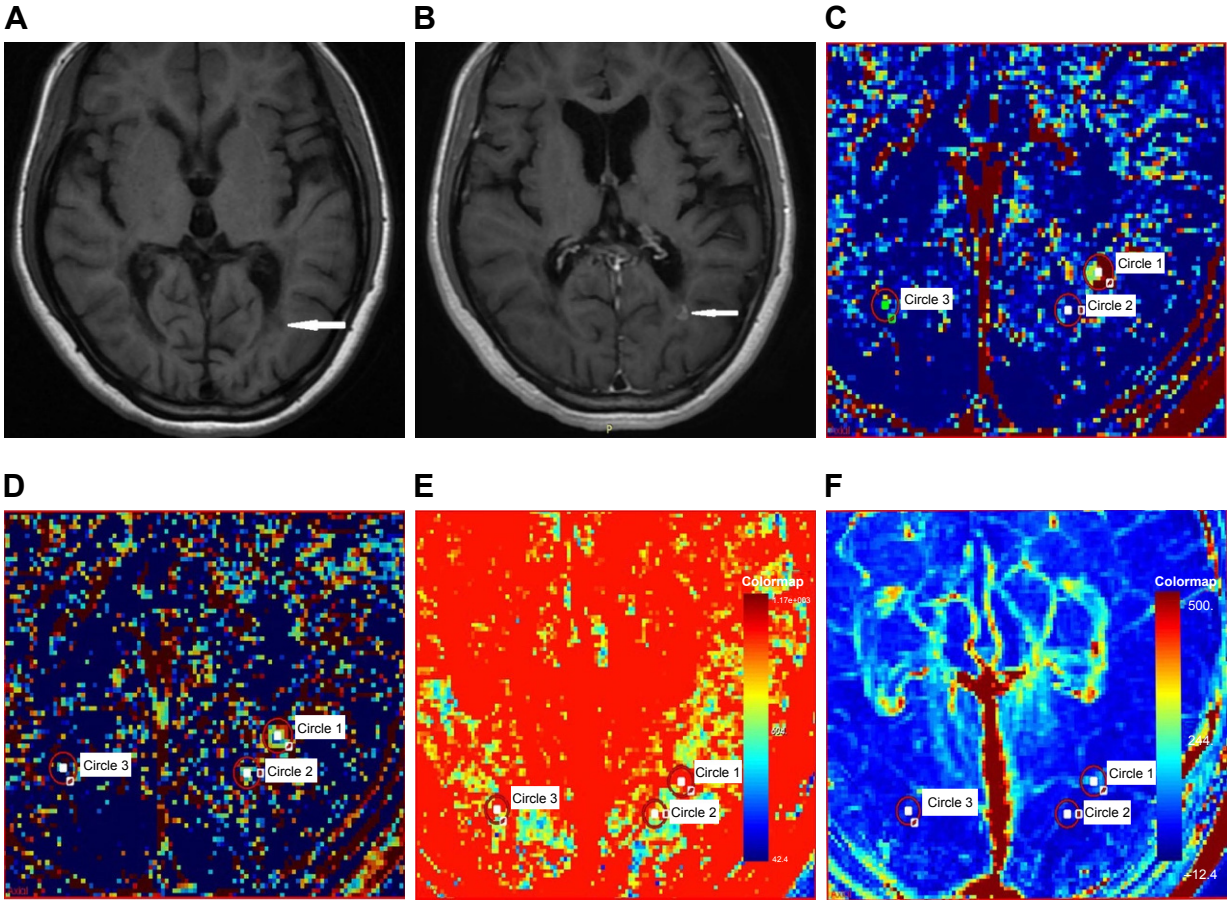

Figure 2 The representative images of dynamic contrast-enhanced magnetic resonance imaging with Patlak model.
Notes: A 24-year-old patient with RRMS. (**A**) Precontrast T1-weighted: round low signal in the left periventricular areas (arrow). (**B**) Dynamic contrast-enhanced T1-weighted images: the lesion was enhanced in T1-weighted contrast-enhanced sequences (arrow). (**C**) K^{trans} map. (**D**) V_p map. (**E**) CBF map. (**F**) CBV map. ROI 1 located in CE lesions (Circle 1), ROI 2 located in the NAWM regions close to the lesions (Circle 2), ROI 3 located in the NAWM regions far from the lesions (Circle 3). For the color maps (**C**–**F**), red color represents a high value, blue color represents a low value.
Abbreviations: CBF, cerebral blood flow; CBV, cerebral blood volume; K^{trans}, volume transfer constant; NAWM, normal-appearing white matter; ROI, region of interest; RRMS, relapsing–remitting multiple sclerosis; V_p, fractional plasma volume.

For CE lesions, the skewness and kurtosis of K^{trans} were significantly higher than those of NE lesions ($P<0.05$, Figure 3, Table 2). This indicated that the skewness of K^{trans} in CE lesions increased to the right side of histogram. In contrast, the skewness of K^{trans} in NE lesions was more close to 0, indicating K^{trans} histogram in NE lesions was more close to normal distribution. Furthermore, the skewness of V_p, CBF, and CBV in NE lesions had no significant difference compared with CE lesions ($P>0.05$, Figure 2D–F, Table 2). In our study, the kurtosis of K^{trans} in NE lesions showed lighter tail compared with CE lesions. However, the kurtosis of V_p, CBF, and CBV in NE lesions had no significant differences compare with CE lesions ($P>0.05$, Table 2, Figure 4).

Table 1 The permeability and perfusion characteristic of MS lesions and NAWM regions

Index	CE	NE	Near NAWM	Far NAWM	χ^2 value	*P*-value
K^{trans}	0.2148 (0.0488–0.4525)	0.0326 (0.0195–0.0716)	0.0456 (0.0195–0.0716)	0.0456 (0.0195–0.0781)	26.847	0.000
V_p	0.2448 (0.1758–0.3626)	0.0352 (0.0195–0.0768)	0.0273 (0.0143–0.0468)	0.0299 (0.0143–0.0508)	64.271	0.000
CBF	45.5483 (32.9309–61.3355)	6.8000 (4.3279–11.4639)	6.0588 (4.3205–11.2014)	6.272 (4.4487–10.4447)	69.547	0.000
CBV	39.787 (29.0745–61.6703)	5.8584 (4.0404–10.9631)	5.1239 (4.1287–9.9228)	5.1210 (4.0478–9.4874)	68.930	0.000

Notes: Median (P_{25}–P_{75}) was used to describe the permeability and perfusion characteristic of MS lesions and NAWM regions. Near NAWM: NAWM regions close to lesions. Far NAWM: NAWM regions far from the lesions. K^{trans}: min^{-1}, V_p: (mL·100 g^{-1}), CBF: (mL·100 g^{-1}·min^{-1}), CBV: (mL·100 g^{-1}).
Abbreviations: CBF, cerebral blood flow; CE, contrast-enhancing; CBV, cerebral blood volume; K^{trans}, volume transfer constant; MS, multiple sclerosis; NAWM, normal-appearing white matter; NE, non-enhancing; V_p, fractional plasma volume.

Table 2 The histogram parameters of MS lesions

	CE	NE	*Z* value	*P*-value
K^{trans}				
Skewness	0.6496 (0.0261 – 1.0477)	0.0389 (–0.2269 to 0.4843)	–2.149	0.032
Kurtosis	–0.4065 (–0.8203 to 0.8362)	–0.7569 (–1.1224 to –0.1806)	–1.982	0.048
V_p				
Skewness	–0.0338 (–0.2137 to 0.6700)	0.2865 (0.0198 – 0.6297)	–1.122	0.262
Kurtosis	–0.8759 (–1.0820 to 0.1161)	–0.7647 (–1.0969 to –0.1817)	–0.024	0.981
CBF				
Skewness	0.1264 (–0.1465 to 0.5258)	0.2588 (–0.1471 to 0.5421)	–0.215	0.830
Kurtosis	–0.9235 (–1.2924 to –0.5948)	–0.7392 (–1.0720 to –0.0897)	–1.408	0.159
CBV				
Skewness	0.2741 (–0.0058 to 0.5472)	0.2262 (0.0333 – 0.4631)	–0.382	0.702
Kurtosis	–0.8579 (–1.2466 to –0.4580)	–0.7682 (–1.1318 to –0.1271)	–0.812	0.417

Notes: Median (P_{25}–P_{75}) was used to describe the histogram characteristic of MS lesions. The Mann–Whitney *U* test in SPSS 21 software was used to compare the differences of these parameters.
Abbreviations: CBF, cerebral blood flow; CE, contrast-enhancing; CBV, cerebral blood volume; K^{trans}, volume transfer constant; MS, multiple sclerosis; NE, non-enhancing; V_p, fractional plasma volume.

Discussion

In our study, abnormalities of cerebral permeability and perfusion in RRMS were quantified using DCE-MRI with Patlak model. The MRI biomarkers K^{trans}, V_p, CBF, and CBV of CE lesions were significantly higher than those of NE lesions and NAWM. The histogram parameters of K^{trans} in NE lesions were more close to 0; these parameters could be helpful to distinguish the CE lesions from NE lesions in MS. The kurtosis of K^{trans} in NE lesions showed more flat and decreased peak height, thereby prompting that the peak of NE lesions was lower than those of normal distribution. However, there were no significant correlations among the K^{trans}, V_p, CBF, and CBV with EDSS scores and disease duration.

The significant increase of K^{trans}, V_p, CBF, and CBV in CE lesions compared with NE lesions and the NAWM regions is consistent with previous findings.[11,12,22] The increased cerebral perfusion CE lesions could be explained by the existence of vasodilation in the lesions. Studies[6,9,11,22] have showed that the pathological processes of MS mainly include inflammatory demyelination, axonal loss, and glial scar formation, and the pathological changes can vary from different lesions. The pathological changes of CE lesions mainly include destruction of the axon, the proliferation of glial cells, ischemic changes in the center, and compensatory dilation of blood vessels around the lesions.[6,11] Nevertheless, we found no significant difference in terms of K^{trans} between NE lesions and NAWM regions, which is consistent with previous study.[23] Cramer et al[4] found a slightly higher K^{trans} value of NAWM regions than our results, while Ingrisch et al reported a similar value with our study.[12] The different sampling time and the pathological changes of NE lesions and NAWM regions may be of importance for the variations of K^{trans} in MS.[11]

Our results also demonstrated that the CBF and CBV of NE lesions were slightly higher than NAWM regions, which is consistent with previous studies.[9,10] Structural changes, including local demyelination of lesions and axonal damage extension into the NAWM regions, axonal swelling, and increased numbers of enlarged microglia were observed in NAWM regions.[6,7,24] Bester et al[8] reported the abnormality of perfusion characteristics of NAWM regions in MS. Although previous studies[21,25] have showed that pathological

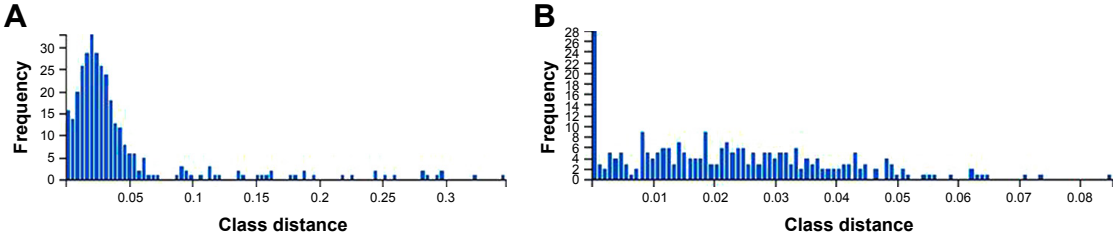

Figure 3 The histogram of K^{trans} in CE lesions (**A**) and NE lesions (**B**).
Note: The skewness of K^{trans} in CE lesions increased to the right side of histogram, while the histogram of K^{trans} in NE lesions was more close to normal distribution.
Abbreviations: CE, contrast-enhancing; K^{trans}, volume transfer constant; NE, non-enhancing.

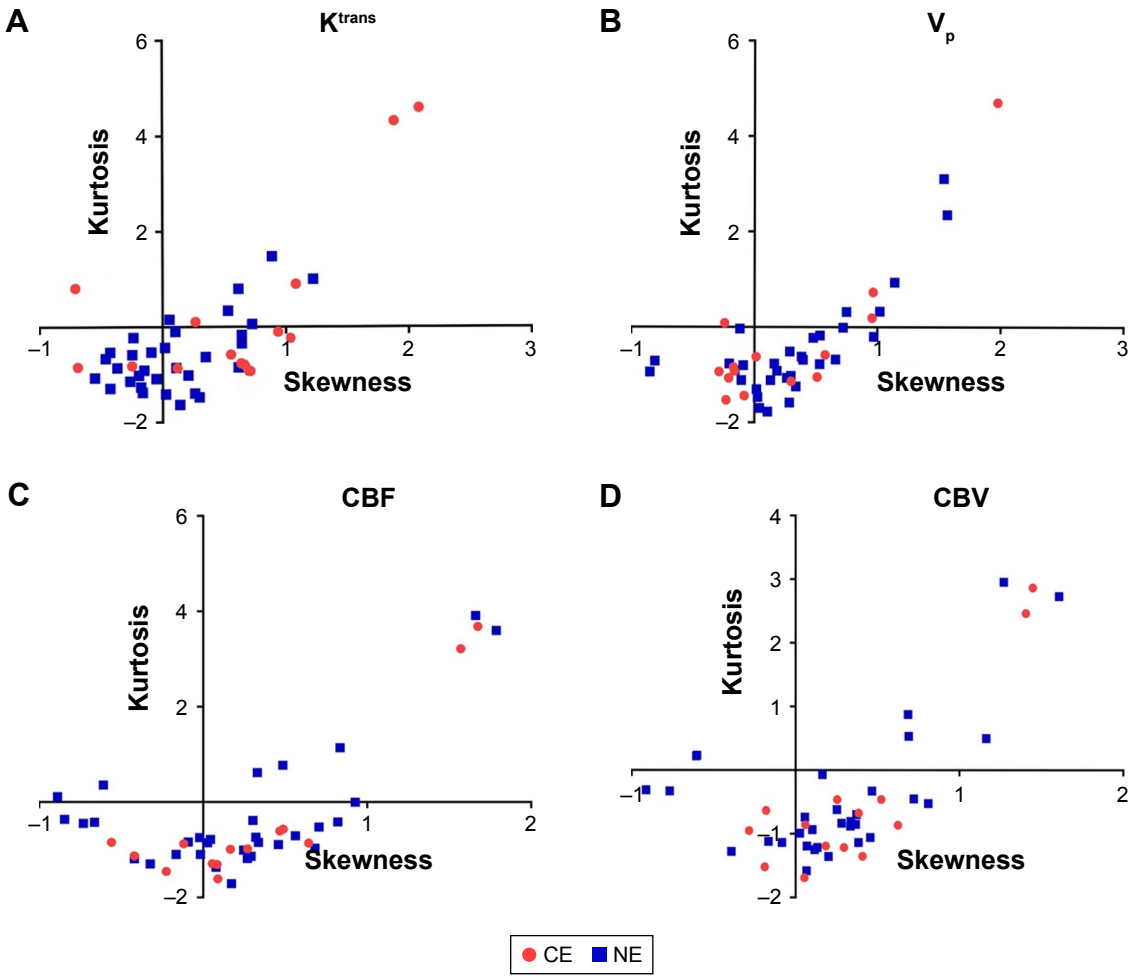

Figure 4 The skewness and kurtosis of different parameters.
Note: The skewness and kurtosis of K^{trans} in CE lesions were significantly higher than NE lesions (**A**), while no significant differences were found in terms of V_p, CBF, and CBV (**B**–**D**).
Abbreviations: CBF, cerebral blood flow; CE, contrast-enhancing; CBV, cerebral blood volume; K^{trans}, volume transfer constant; NE, non-enhancing; V_p, fractional plasma volume.

changes of NAWM areas varied from the distance between lesions, we found no significant difference of permeability and perfusion parameters between NAWM regions close to lesions and NAWM regions far from the lesions. This may be attributed to the fact that the majority of lesions in our study were not in the active stage. Furthermore, correlation analysis shows that the permeability and perfusion parameters have no significant associations with clinical disability status and disease duration. This could be related to the reconstitution after inflammatory activity, which may limit clinical manifestations. In addition, the small sample size may be responsible for this situation.[26]

Previous studies have reported that the skewness and kurtosis were useful parameters and significantly sensitive to small changes or treatment effects.[13,27–29] In this study, we found that the skewness and kurtosis of K^{trans} in CE lesions were significantly higher than NE lesions. This indicated that the skewness of K^{trans} in CE lesions increased to the right side of histogram, while the skewness of K^{trans} in NE lesions were more close to 0, indicating that K^{trans} in NE lesions were more close to normal distribution. So we believe that the aforementioned histogram parameters of K^{trans} can be used to distinguish CE lesions from NE lesions, especially when the enhancement is not obvious or visible on post contrast T1 weighted in clinical practice. However, this result should be cautiously explained because CE lesions are very heterogeneous by nature. These lesions have more heterogeneous pharmacokinetic values compared with NE lesions usually due to the difference of interval between lesion onset and MRI scanning.

Limitations of this study should be mentioned. First, our results should be interpreted with caution because of the small sample size. Although previous study[12] has investigated the feasibility of quantification of the cerebral permeability and

perfusion changes by performing even less patients, further studies should be conducted in a larger sample size. Second, our study had a cross-sectional design, longitudinal studies are necessary to determine whether permeability and perfusion parameters change dynamically. Third, DCE-MRI is the only modality used for measuring permeability and perfusion changes; so, more methods should be assessed. Finally, due to a relatively short total measurement time for DCE-MRI, a lower accuracy may be obtained.

In conclusion, our study demonstrated that DCE-MRI with Patlak model can quantitatively measure the permeability and perfusion characteristics in MS lesions and NAWM regions. The K^{trans}, V_p, CBF, and CBV of CE lesions were significantly higher than those of NE lesions. No significant difference was found among these parameters between NE lesions and NAWM regions. There was no significant difference of permeability and perfusion parameters between NAWM regions close to lesions and NAWM regions far from the lesions. In addition, we observed that the histogram parameters of CE and NE lesions in MS were different from each other, indicating that the histogram parameters can be helpful to distinguish the pathology of MS lesions. Interestingly, we found no correlation among the K^{trans}, V_p, CBF, and CBV with EDSS scores and disease duration in MS lesions.

Acknowledgments

This study was supported by the Medical Research Key Program of the National Health and Family Planning Commission of Chongqing, China (No 20141016 and No 2016ZDXM026), the Basic and Frontier Research Project of Chongqing, China (No cstc2016jcyjA0294), and the Scientific and Technological Innovation Project of Chongqing General Hospital, University of Chinese Academy of Sciences (No 2016ZDXM03). The authors thank EzPubedit (http://ezpubedit.com) for linguistic assistance during the preparation of this manuscript.

Disclosure

The authors report no conflicts of interest in this work.

References

1. Yuan J, Chow SK, Zhang Q, Yeung DK, Ahuja AT, King AD. The use of dynamic tracer concentration in veins for quantitative DCE-MRI kinetic analysis in head and neck. *PLoS One*. 2013;8(3):e59885.
2. Bergamino M, Bonzano L, Levrero F, Mancardi GL, Roccatagliata L. A review of technical aspects of T1-weighted dynamic contrast-enhanced magnetic resonance imaging (DCE-MRI) in human brain tumors. *Phys Med*. 2014;30(6):635–643.
3. Larsson HB, Stubgaard M, Frederiksen JL, Jensen M, Henriksen O, Paulson OB. Quantitation of blood-brain barrier defect by magnetic resonance imaging and gadolinium-DTPA in patients with multiple sclerosis and brain tumors. *Magn Reson Med*. 1990;16(1):117–131.
4. Cramer SP, Larsson HB. Accurate determination of blood-brain barrier permeability using dynamic contrast-enhanced T1-weighted MRI: a simulation and in vivo study on healthy subjects and multiple sclerosis patients. *J Cereb Blood Flow Metab*. 2014;34(10):1655–1665.
5. Tofts PS, Kermode AG. Measurement of the blood-brain barrier permeability and leakage space using dynamic MR imaging. 1. Fundamental concepts. *Magn Reson Med*. 1991;17(2):357–367.
6. Stadelmann C, Wegner C, Brück W. Inflammation, demyelination, and degeneration – recent insights from MS pathology. *Biochim Biophys Acta*. 2011;1812(2):275–282.
7. Lund H, Krakauer M, Skimminge A, et al. Blood-brain barrier permeability of normal appearing white matter in relapsing-remitting multiple sclerosis. *PLoS One*. 2013;8(2):e56375.
8. Bester M, Forkert ND, Stellmann JP, et al. Increased perfusion in normal appearing white matter in high inflammatory multiple sclerosis patients. *PLoS One*. 2015;10(3):e0119356.
9. Ge Y, Law M, Johnson G, et al. Dynamic susceptibility contrast perfusion MR imaging of multiple sclerosis lesions: characterizing hemodynamic impairment and inflammatory activity. *ANJR Am J Neuroradiol*. 2005;26(6):1539–1547.
10. Law M, Saindane AM, Ge Y, et al. Microvascular abnormality in relapsing-remitting multiple sclerosis: perfusion MR imaging findings in normal-appearing white matter. *Radiology*. 2004;231(3):645–652.
11. Kipp M, van der Valk P, Amor S. Pathology of multiple sclerosis. *CNS Neurol Disord Drug Targets*. 2012;11(5):506–517.
12. Ingrisch M, Sourbron S, Morhard D, et al. Quantification of perfusion and permeability in multiple sclerosis: dynamic contrast-enhanced MRI in 3D at 3T. *Invest Radiol*. 2012;47(4):252–258.
13. Patlak CS, Blasberg RG, Fenstermacher JD. Graphical evaluation of blood-to-brain transfer constants from multiple-time uptake data. *J Cereb Blood Flow Metab*. 1983;3(1):1–7.
14. Alcaide-Leon P, Rovira À. Dynamic contrast-enhanced MR: importance of reaching the washout phase. *Am J Neuroradiol*. 2013;34(5):E58–E59.
15. Just N. Improving tumour heterogeneity MRI assessment with histograms. *Br J Cancer*. 2014;111(12):2205–2213.
16. Shukla-Dave A, Lee NY, Jansen JF, et al. Dynamic contrast-enhanced magnetic resonance imaging as a predictor of outcome in head-and-neck squamous cell carcinoma patients with nodal metastases. *Int J Radiat Oncol Biol Phys*. 2012;82(5):1837–1844.
17. Kim H, Choi SH, Kim JH, et al. Gliomas: application of cumulative histogram analysis of normalized cerebral blood volume on 3 T MRI to tumor grading. *PLoS One*. 2013;8(5):e63462.
18. Thompson AJ, Banwell BL, Barkhof F, et al. Diagnosis of multiple sclerosis: 2017 revisions of the McDonald criteria. *Lancet Neurol*. 2018;17(2):162–173.
19. Lavini C, Verhoeff JJ. Reproducibility of the gadolinium concentration measurements and of the fitting parameters of the vascular input function in the superior sagittal sinus in a patient population. *Magn Reson Imaging*. 2010;28(10):1420–1430.
20. Heye AK, Thrippleton MJ, Armitage PA, et al. Tracer kinetic modelling for DCE-MRI quantification of subtle blood-brain barrier permeability. *Neuroimage*. 2016;125:446–455.
21. Moll NM, Rietsch AM, Thomas S, et al. Multiple sclerosis normal-appearing white matter: pathology-imaging correlations. *Ann Neurol*. 2011;70(5):764–773.
22. Yin P, Xiong H, Liu Y, et al. Measurement of the permeability, perfusion, and histogram characteristics in relapsing-remitting multiple sclerosis using dynamic contrast-enhanced MRI with extended Tofts linear model. *Neurol India*. 2018;66(3):709–715.
23. Cramer SP, Simonsen H, Frederiksen JL, Rostrup E, Larsson HB. Abnormal blood-brain barrier permeability in normal appearing white matter in multiple sclerosis investigated by MRI. *Neuroimage Clin*. 2014;4:182–189.
24. Wegner C. Recent insights into the pathology of multiple sclerosis and neuromyelitis optica. *Clin Neurol Neurosurg*. 2013;115(Suppl 1):S38–S41.

25. Vrenken H, Geurts JJ. Gray and normal-appearing white matter in multiple sclerosis: an MRI perspective. *Expert Rev Neurother*. 2007;7(3):271–279.
26. Vrenken H, Geurts JJ, Knol DL, et al. Normal-appearing white matter changes vary with distance to lesions in multiple sclerosis. *AJNR Am J Neuroradiol*. 2006;27(9):2005–2011.
27. Rumzan R, Wang JJ, Zeng C, et al. Iron deposition in the precentral grey matter in patients with multiple sclerosis: a quantitative study using susceptibility-weighted imaging. *Eur J Radiol*. 2013;82(2):e95–e99.
28. Hayes C, Padhani AR, Leach MO. Assessing changes in tumour vascular function using dynamic contrast-enhanced magnetic resonance imaging. *NMR Biomed*. 2002;15(2):154–163.
29. Peng SL, Chen CF, Liu HL, et al. Analysis of parametric histogram from dynamic contrast-enhanced MRI: application in evaluating brain tumor response to radiotherapy. *NMR Biomed*. 2013;26(4):443–450.